JOURNAL OF MATERIALS SCIENCE 32 (1997) 245–258

# Synthesis and study of organically capped ultra small clusters of cadmium sulphide

M. KUNDU, A. A. KHOSRAVI, S. K. KULKARNI
*Centre for Advanced Studies in Materials Science, Department of Physics, University of Poona, Pune 411 007, India*

P. SINGH
*National Chemical Laboratory, Pashan, Pune 411 008, India*

Ultra small clusters of cadmium sulphide are synthesized using non-aqueous and aqueous chemical methods. Thiophenol has been used as a capping agent for non-aqueous synthesis whereas various reagents such as mercaptoethanol, hexametaphosphate, ethylene glycol and ethanol have been used as additives for an aqueous method of synthesis. Properties of the clusters synthesized are discussed based on optical absorption, X-ray diffraction, transmission electron diffraction and photoelectron spectroscopy. Particles as small as $\sim 0.7$ nm diameter could be synthesized with thiophenol and mercaptoethanol as additives. The effect of varying the molarities of the different additives on the properties of the CdS nanoclusters synthesized are discussed. Systematic ageing studies of the nanoclusters showed that larger particles age faster than the smaller clusters. Ageing also leads to better crystallization of the particles. It has been observed that the smallest particles ($\sim 0.7$ nm diameter) possess tetrahedrally bonded fragments of CdS and intercluster structural long range order does not exist. However, bigger particles ($\sim 2.0$ nm diameter) show bulk cubic structure. X-ray photoelectron spectroscopy studies have been done to study the purity and stoichiometry of the clusters synthesized and strongly support the existing proposal of the formation and stability of CdS nanoclusters.

## 1. Introduction

Semiconductor nanoparticles with diameters less than about 10 nm, now widely known as "quantum dots", are the subject of intense investigations [1–9]. The number of atoms in such quantum dots ranges from a few tens to hundreds of atoms and are truly clusters of atoms with properties intermediate to those of molecules and bulk materials. Such clusters of atoms exhibit exotic phenomena of size effect with unique electronic and optical properties that depend upon the size of the cluster. The surface to bulk atom ratio also changes rapidly with size leading to drastic changes in thermal and mechanical properties. The technological potential of semiconductor quantum dots in photocatalysis, solar energy conversion, non-linear optical devices, etc., has been well realized [10–12]. However, to achieve the desired properties it is essential to obtain proper control of the particle size. Usually nuclei of desired material are grown to the required size and encapsulated by means of some organic molecules or trapped in media-like polymers or zeolites in order to avoid agglomeration or coalescence of the clusters [5, 13–14]. Other methods, using inverse micelle [15–18] and silicate glass [19–21] as host materials for the synthesis of semiconductor clusters, have also been used. Amongst these methods, a chemical route, in which the nanosized clusters are capped with organic materials, has a distinct advantage over the other methods. By this method the free standing clusters of semiconductors can be easily formed in large quantities by relatively inexpensive means.

The chemical route can be divided into non-aqueous and aqueous methods of synthesis. Herron *et al.* [5] have used the ideas proposed by Dance and coworkers [22] of surface capping of CdS using thiophenol (non-aqueous method) and obtained powders of II–VI semiconductors. They have done chemical and NMR analysis along with XRD and optical absorption studies to arrive at the correlation between cluster size and phenyl group concentration. Cluster size effects in CdS can be observed very prominently for radius $< 3$ nm which is the Bohr radius of exciton for this material. Nosaka and his group [23] have synthesized CdS clusters by the aqueous method using various additives. They studied the change in the optical absorption spectra and the quantum yield of photoinduced electron transfer for the size controlled CdS colloids. In this work we have synthesized CdS clusters by non-aqueous (thiophenol capping) as well as aqueous methods (by using different additives). We present here the systematic studies of CdS cluster synthesis and characterization. We have tried to

0022–2461  

investigate effects of various solution parameters of the constituents in the reaction which would enable quickly to obtain clusters of desired properties.

## 2. Experimental

Chemical synthesis of CdS quantum dots has been performed by non-aqueous as well as aqueous methods. The non-aqueous method of synthesis used was initially suggested by Herron and co-workers [5]. Here cadmium acetate ($Cd(CH_3COO)_2$) and sodium sulphide ($Na_2S$) were used as starting materials. Thiophenol (SPh) was used as an organic additive which acts as a capping agent. $Na_2S$ was placed in a reaction vessel and stirred continuously. To this the additive thiophenol was added drop by drop. Finally cadmium acetate was added very slowly into it. The solution obtained was centrifuged and the precipitate thus obtained was washed thoroughly in methanol 4–5 times to remove any unreacted, excess $Na_2S$ or thiophenol which might be present. The precipitate was air dried. Free standing particles were obtained under different S/SPh ratios. S/SPh ratio is the concentration of sulphur in $Na_2S$ to the concentration of thiophenol.

CdS nanoclusters were synthesized by the aqueous method similar to that followed by Nosaka *et al.* [23]. Synthesis of CdS clusters using various capping agents was done. $CdCl_2$ and $Na_2S$ were used as starting materials. The additives used were mercaptoethanol ($C_2H_5SH$ or RSH), sodium hexametaphosphate ($(NaPO_3)_6$ or HMP), ethylene glycol ($C_2H_4(OH)_2$ or EG) and ethanol ($C_2H_5OH$ or E). Experiments were also performed by varying the molarity of the additives to obtain changes in the physical properties of the nanoclusters. The experimental procedure was similar to the non-aqueous method of synthesis of clusters. The solution obtained as end product was centrifuged and the precipitate obtained was washed in double distilled water 4–5 times to remove excess $Na_2S$ which might be present.

CdS nanoclusters obtained by non-aqueous as well as aqueous method were characterized by optical absorption, X-ray diffraction (XRD), transmission electron microscopy (TEM) and X-ray photoelectron spectroscopy (XPS).

Optical absorption studies were made on a Hitachi 303 double beam spectrophotometer. The CdS powders were dissolved in acetonitrile medium and double distilled water for clusters synthesized by non-aqueous and aqueous methods, respectively.

Samples in the form of powder were spread on $SnO_2$ coated glass slides in acetonitrile (non-aqueous) and double distilled water (aqueous) medium. After drying, the sample was introduced into the ultra high vacuum chamber ($\sim 10^{-9}$ torr) for photoelectron spectroscopy.

XPS of all the CdS quantum dot powders could be carried out without any problems as the samples were vacuum and radiation stable. XPS was carried out in a VG Scientific U.K. ESCALAB MkII system. $AlK_\alpha$ (1486.6 eV) was used as a source of radiation. A concentric hemispherical analyser with 20 eV pass energy

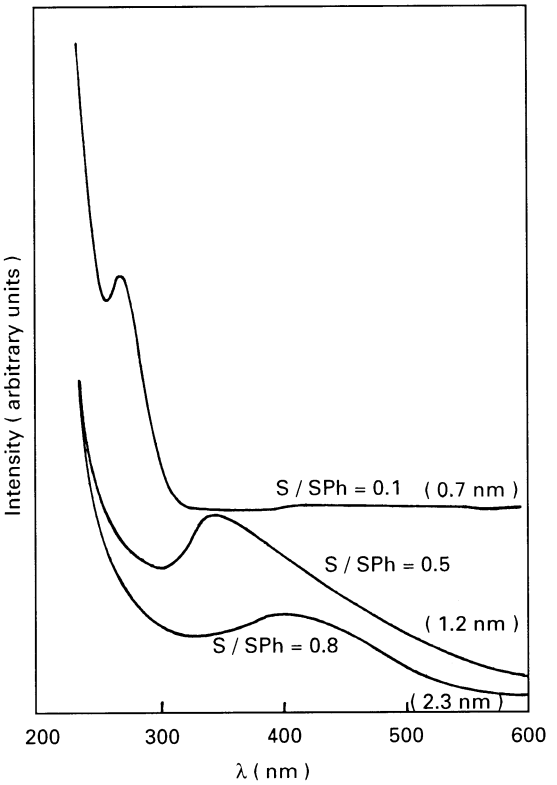


*Figure 1* Optical absorption spectra for the thiophenol capped CdS clusters with various S/SPh ratios.

was used as the photoelectron kinetic energy analyser. The resolution was $\sim 0.9$ eV and accuracy of $\pm 0.2$ eV was obtained. The data were collected on a computerized data acquisition system in order to process it for detailed analysis. Due to the charging effect C 1s itself at 285.0 eV was taken as the reference. The external reference was Au $4f_{7/2}$ at 84.0 $\pm$ 0.2 eV.

XRD studies of dry samples were done using a Philips PW1840 powder X-ray diffractometer with $CuK_\alpha$ ($\lambda = 1.542$ A°) as the source of radiation. The samples were prepared on a glass slide using the same procedure as described above for XPS.

TEM was performed using JEOL model 1200 Ex operated at 100 kV. The CdS samples for electron diffraction were obtained by dispersing the powder on a carbon film supported over a specimen grid.

## 3. Results and discussion

### 3.1. CdS nanoclusters obtained by non-aqueous method

In this case thiophenol was used as an additive for controlling the particle size by capping the clusters with the phenyl group of the thiophenol. Wang and Herron [24] have observed that the CdS clusters consist of cores which are essentially CdS but whose surfaces are covered by phenyl groups.

Fig. 1 illustrates the results for thiophenol capped CdS clusters where optical absorption has been shown as a function of wavelength. It can be readily seen that as the S/SPh ratio reduces, i.e. the thiophenol concentration increases, the excitonic peak progressively shifts to the shorter wavelength as well as becoming sharper. This is an indication of a narrow size

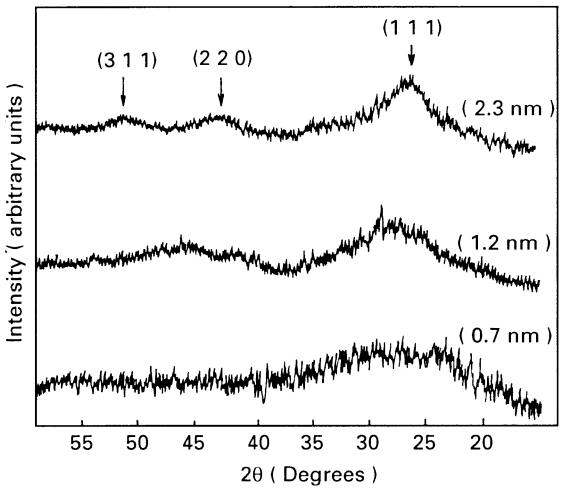


*Figure 2* X-ray diffraction patterns for the various CdS clusters obtained with thiophenol as the additive.

distribution, increase in the bandgap and creation of a sharp excitonic level. Wang and Herron [9, 24] also obtained CdS clusters using thiophenol as the capping agent. Optical absorption spectra showed a sharp feature at 275 nm for 0.7 nm clusters and as the cluster size increased the sharpness of the excitonic peak reduced with a decrease in bandgap, which is similar to our results. However, as discussed at a later stage, we carried out XPS studies of the CdS nanoclusters to understand the electronic structure as well as purity and stoichiometry of the nanoclusters synthesized.

Fig. 2 shows the X-ray diffractograms for the various CdS quantum dot powders obtained by the variation of S/SPh ratio. The estimated cluster size of the particles was obtained using the Scherrer formula [25], namely

$$d' = \frac{0.9\lambda}{\beta\cos\theta} \quad (1)$$

where $\lambda$ is the wavelength of the incident radiation, $\beta$ is the full width at half maximum and $\theta$ is the peak position. In fact the sizes mentioned in Fig. 1 are those derived from X-ray diffractograms in Fig. 2. Particle sizes of 0.7, 1.2 and 2.3 nm were obtained. Table I lists the wavelengths of the excitonic peaks, the optical bandgap of the CdS quantum dots and the corresponding particle sizes with the variation of S/SPh ratio. The results are in agreement with those reported earlier [5, 24] that reduction in S/SPh ratio leads to reduction in cluster diameter. However these conclusions by Herron and co-workers [5] were based on NMR studies. It was shown that the coverage of the capping agent thiophenol increases with decreasing cluster size and is effective in passivation [24, 26].

TABLE I Particle size and optical bandgap of CdS clusters obtained by the variation of S/SPh ratio

| S/SPh molarity ratio | Wavelength λ (nm) | Optical band gap (eV) | Particle size (nm) estimated by XRD |
|---|---|---|---|
| 0.83 | 410 | 3.02 | 2.3 |
| 0.5 | 345 | 3.59 | 1.2 |
| 0.1 | 270 | 4.59 | 0.7 |

We have carried out photoelectron spectroscopy studies which essentially lead to similar results. A composition analysis has been made with a view that in semiconducting materials purity plays an important role. In Table II we have given the concentration of observed elements along with C/S, C/Cd and S/Cd ratios.

The survey scans of the CdS cluster powder samples are illustrated in Fig. 3. It is evident that there are no impurities present except for a small amount of oxygen. In fact the C/S ratio slightly increases and the oxygen amount reduces with reduction in cluster size. This is an indication of better passivation for small clusters due to more phenyl groups being attached to them. The S/Cd and C/Cd ratio increases with cluster size reduction. It was proposed by Herron *et al.* [5] that the smallest 0.7 nm clusters are probably $[Cd_{10}S_4(SPh)_{16}]$ molecules with a pyramid shape. The expected atomic ratio for S/Cd would be 2.0 and C/Cd would be 9.6 for such a molecule, which are close to those observed by us (Table II). We obtained less sulphur and more carbon than expected.

The molecular structure shown in [22] for $[Cd_{10}S_4(SPh)_{16}]$ exhibits ten spharelite-like CdS units and sixteen phenyl groups attached to sulphur on the boundary of the pyramid structure. Thus covalent bonding of the bulk CdS crystal is maintained, although bond lengths vary substantially [22]. However the smallest unit is not a cube nor do we expect inter-cluster structural long range order. It is not surprising to observe that the electron diffraction pattern for the smallest synthesized cluster, as shown in Fig. 4a exhibits a diffused ring characteristic of an amorphous sample and the sharpness of the diffraction rings increases for 1.2 and 2.3 nm clusters (Fig. 4b and c, respectively). Selected area diffraction patterns for 1.2 and 2.3 nm clusters are shown in Fig. 5a and b. The cubic structure of CdS clusters can be easily observed. X-ray diffractograms of CdS nanoclusters as

TABLE II Concentration of various elements present in the CdS clusters of various sizes obtained with the additive thiophenol

| S/SPh molarity ratio | Particle size (nm) | Cd (%) | S (%) | C (%) | O (%) | S/Cd | C/Cd | C/S |
|---|---|---|---|---|---|---|---|---|
| Bulk | Bulk | 31.0 | 29.6 | 27.2 | 12.2 | 1.0 | 0.89 | 0.9 |
| 0.83 | 2.3 | 9.4 | 11.2 | 73.6 | 5.5 | 1.2 | 7.82 | 6.5 |
| 0.5 | 1.2 | 8.6 | 11.2 | 77.1 | 3.1 | 1.3 | 8.96 | 6.8 |
| 0.1 | 0.7 | 7.1 | 11.3 | 78.6 | 3.0 | 1.6 | 11.0 | 7.0 |

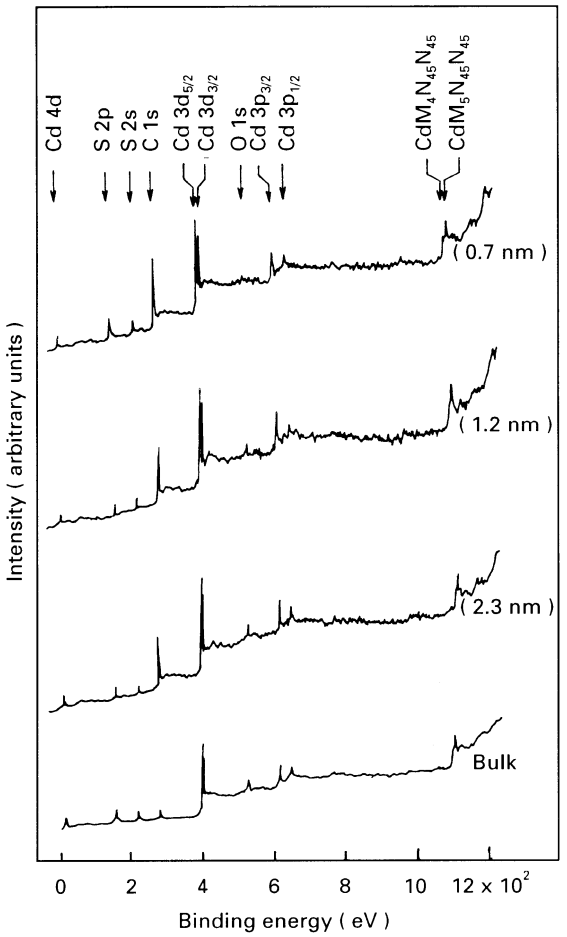


*Figure 3* Survey scan of thiophenol capped CdS clusters of various sizes.

shown in Fig. 2 essentially lead to the same conclusion that the smallest 0.7 nm particle shows an amorphous nature and as the particle size increases, amorphosity reduces and planes characteristic of long range order start appearing. We also note from Fig. 2 that 2.3 nm CdS cluster shows a peak at $2\theta = 26.9^\circ$ which shifts to $2\theta = 28.2^\circ$ for 0.7 nm diameter cluster. The lattice constant for 1.2 and 2.3 nm clusters are 0.565 and 0.579 nm, respectively. This shows that there is a slight decrease in lattice parameter with decrease in cluster size and this qualitatively agrees with that reported earlier for thiophenol capped CdS clusters [22]. The (1 1 1), (2 2 0) and (3 1 1) planes characteristic of cubic CdS phase are clearly observed for 2.3 nm diameter cluster. Obviously the smallest cluster of CdS is not a cube, yet smaller clusters maintain tetrahedral fragments of it.

Interestingly, these local units of CdS still show a systematic correlation with the electronic structure of bulk and characteristic properties of cadmium sulphide. The binding energy positions of Cd $3d_{3/2}$, Cd $3d_{5/2}$ and S 2p core levels are listed in Table III.

In Fig. 6a and b we have plotted Cd 3d and S 2p spectra for various thiophenol capped clusters of CdS and compared those with a bare bulk CdS reference sample. In Fig. 6a it can be observed that there is a small shift of both the peaks of cadmium, i.e. Cd $3d_{3/2}$ and Cd $3d_{5/2}$, to the high binding energy side with decrease in cluster size. In Fig. 6b the S 2p peak also shifts to the higher binding side with reduced cluster size. This is consistent with increasing HOMO–LUMO gap and corresponding shifts of all occupied levels to higher binding energy.

Hence we can say that a blue shift is observed for 0.7, 1.2 and 2.3 nm particle sizes and there is a considerable variation in the properties of very small sized clusters. 0.7 and 1.2 nm diameter clusters possess tetrahedrally bonded fragments of CdS.

## 3.2. CdS nanoclusters obtained by aqueous method

As mentioned earlier, the aqueous method of synthesis is similar to that reported by Nosaka *et al.* [23]. Here cadmium chloride ($CdCl_2$) and sodium sulphide ($Na_2S$) solutions have been used. We used mercaptoethanol (RSH), hexametaphosphate (HMP), ethylene glycol (EG) and ethanol (E) as the additives. Comparative study of the CdS nanoclusters thus obtained was made. Molarity of the additives was kept at 0.5 M. Fig. 7 shows the optical absorption spectra for CdS nanoclusters prepared by using different additives. Variation in physical properties of the clusters with different additives was observed. It was observed that maximum blue shift with respect to bulk CdS was obtained when RSH was used as an additive. Table IV shows the excitonic peak positions and optical bandgap obtained with various additives. It is observed from Fig. 7 that as the optical bandgap becomes large, the excitonic peak becomes sharper. All these observations indicated that a narrow size distribution with increased bandgap and sharper excitonic features is obtained for RSH as the additive. Thus under similar preparation conditions of CdS quantum dots, different additives give rise to different optical bandgaps.

In order to gain further understanding about the synthesis, we performed, as shown in Fig. 8a to d, the synthesis of CdS nanoclusters using various additives (RSH, HMP, EG and E) by varying the molarity of the additives, i.e. 0.5, 0.01 and 0.0001 M. From the experiments carried out it was observed that only with the increase or decrease in the RSH molarity large changes in optical absorption spectra or physical properties of the nanoclusters were obtained. It is obvious that out of these four additives, RSH yielded the smallest sized particles with a narrow size distribution as well as showing the capacity for giving nanoclusters of different sizes. Nosaka *et al.* [23] carried out only optical absorption studies and observed excitonic peaks in the absorption spectra for CdS nanoclusters with the additives described by us. However the optical bandgap of the clusters obtained by us is larger and peaks are sharper and narrow indicating better and uniform size distribution. (A bandgap of 3.93 eV was observed by us as against 3.5 eV by Nosaka and his group [23] for CdS clusters with RSH as the capping agent.) In addition to absorption studies, we carried out XRD, TEM and XPS studies as well, which helps in further understanding the properties of the nanoclusters synthesized. Particle size measurements were done here using X-ray diffraction data.

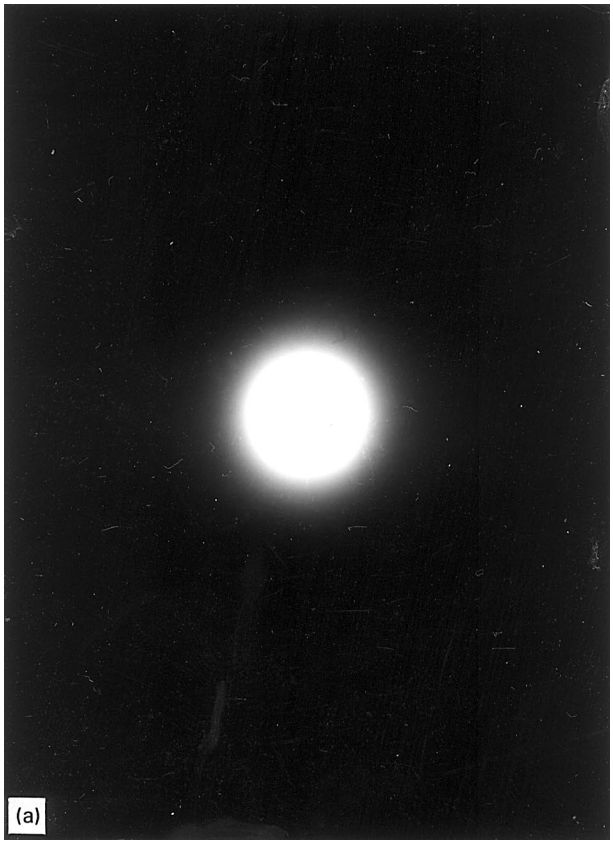


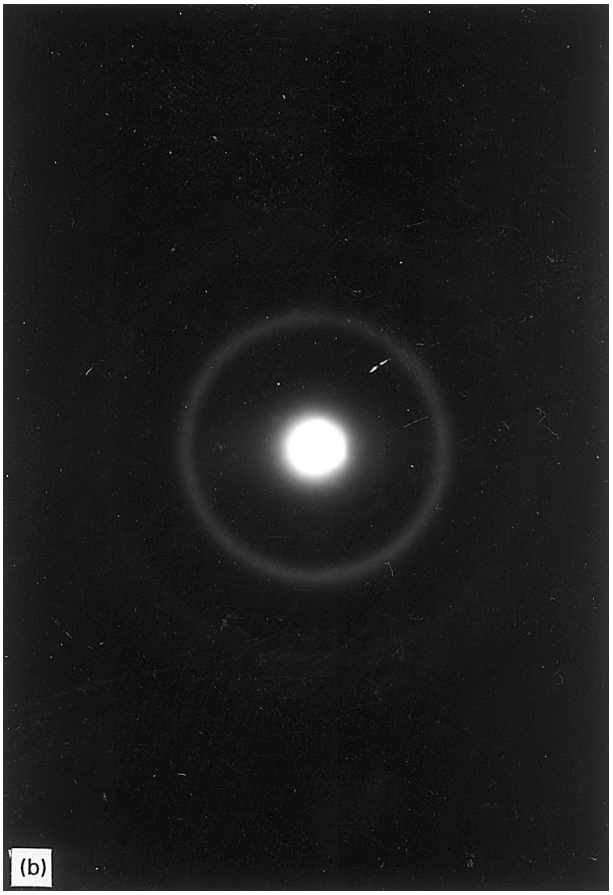


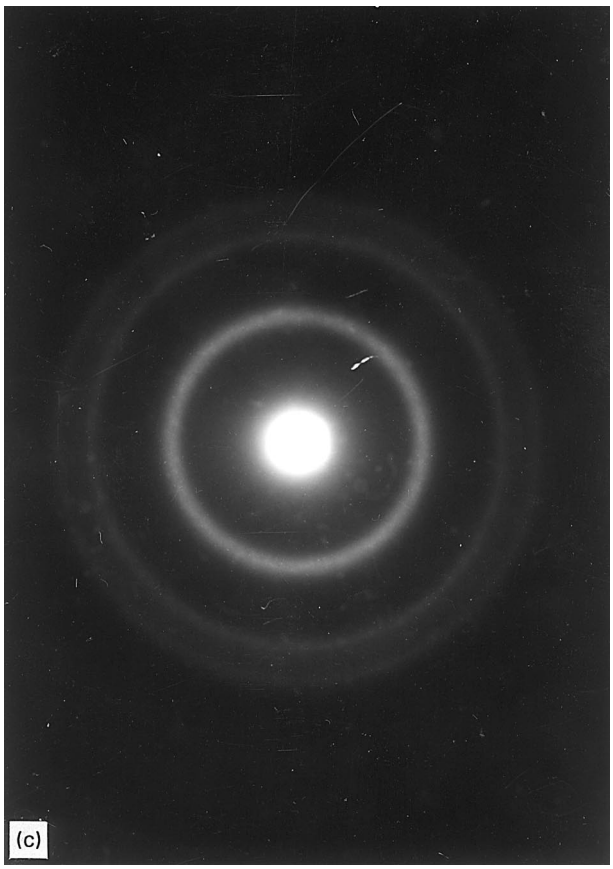


*Figure 4* Electron diffraction patterns for (a) 0.7 nm, (b) 1.2 and 2.3 nm thiophenol capped CdS clusters.

Fig. 9 shows the X-ray diffraction patterns for the CdS clusters obtained by using various additives at a molarity of 0.5 M. Particles size measurements were again done using the Scherrer formula [25]. Particle sizes of 0.8, 1.6, 2.2 and 2.6 nm were obtained with RSH, HMP, EG and E as additives, respectively. This showed that with the same molarity of the various additives used, different particle sizes may be obtained. It is observed from the XRD patterns that with RSH as the additive at 0.5 M (smallest particle) amorphous clusters are obtained. As the cluster size increases, planes characteristic of cubic CdS phase namely (1 1 1), (2 2 0) and (3 1 1) are observed.

For clusters obtained using the aqueous method of synthesis we have again used XPS to confirm the purity and stoichiometry of the samples. As discussed earlier detection of purity for the nanoclusters synthesized is extremely important because if nanoclusters, at the size regime of a few nanometres and containing a few atoms, contain even a very small number of impurity atoms, these may change the properties of the nanoclusters. Fig. 10 gives the survey scan of the CdS quantum dots with various additives. C, Cd, S and O were the elements which could be detected. With hexametaphosphate as the additive, phosphorous was also observed. This is very natural as the phosphate group is present in HMP additive.

Table V gives the percentage of various elements present in the CdS nanoclusters for various particle sizes obtained with different additives. The various rates of C/Cd, S/Cd, and C/S were also tabulated.

It has been shown that thiols like RSH have the property of getting tightly adsorbed on the CdS surface [23, 27]. RSH contains sulphur as one of the elements. Hence S excess CdS nanoparticles are

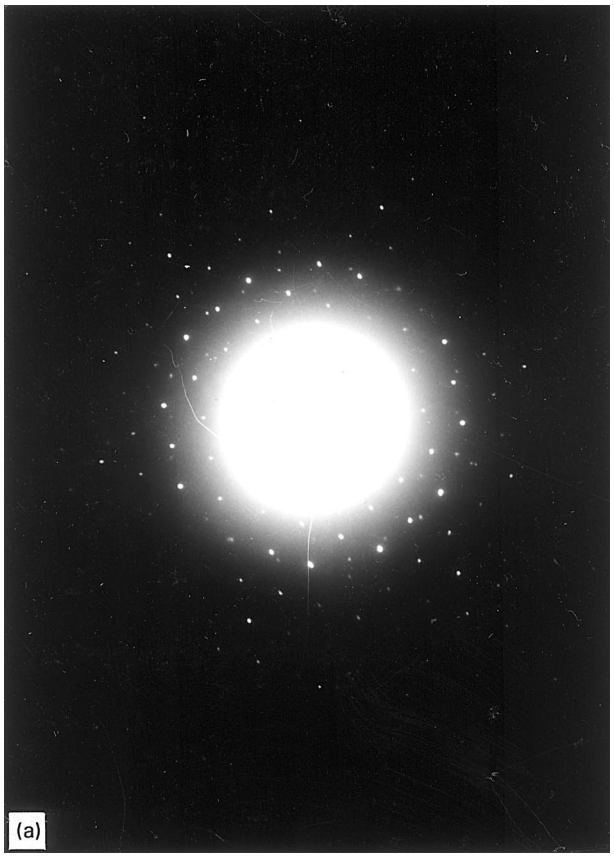


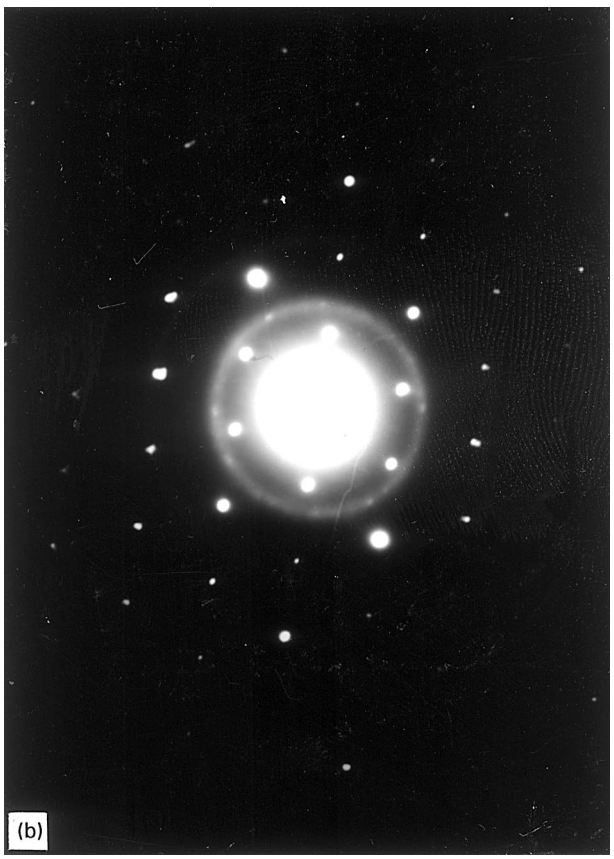


*Figure 5* Selected area diffraction patterns for (a) 1.2 nm and (b) 2.3 nm thiophenol capped CdS clusters.

expected as seen from S/Cd ratio, which is 1.52 for CdS cluster obtained using RSH as the additive. However, as observed from Table V, the S/Cd ratio was 0.82, 0.84 and 0.91 for CdS nanoclusters obtained

TABLE III Cd 3d and S 2p XPS core level positions for CdS clusters of various sizes obtained with thiophenol additive

| Particle size (nm) | Cd 3d $(eV)^{5/2}$ | Cd 3d $(eV)^{3/2}$ | S 2p (eV) |
|---|---|---|---|
| Bulk | 405.3 | 412.1 | 162.1 |
| 2.3 | 405.9 | 412.7 | 162.75 |
| 1.2 | 406.0 | 412.75 | 162.95 |
| 0.7 | 406.0 | 412.75 | 162.95 |

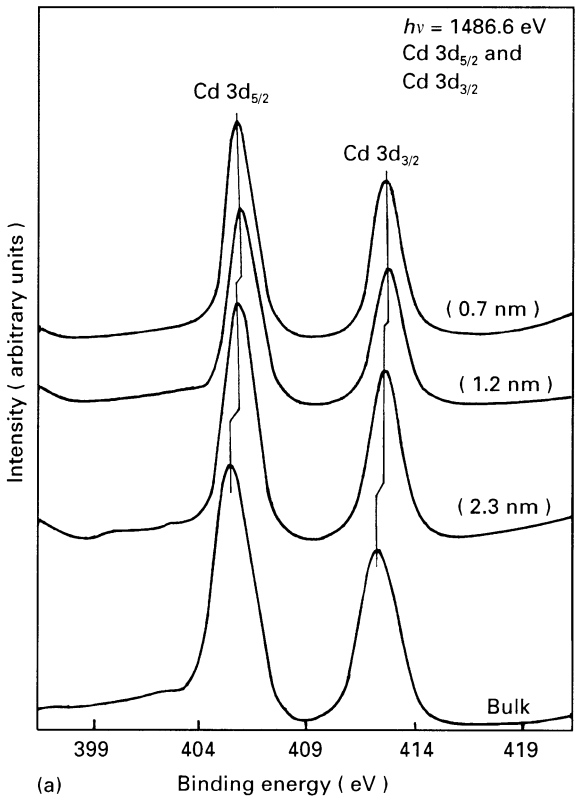


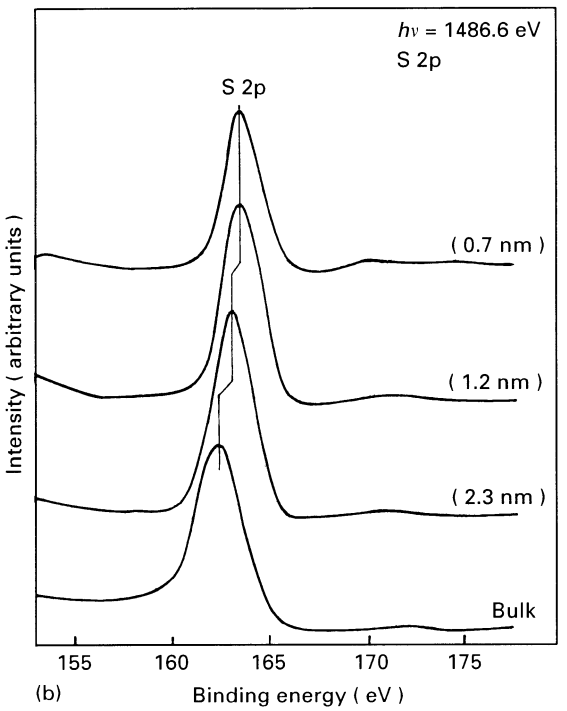


*Figure 6*(a) Cd 3d XPS core level spectra of thiophenol capped CdS clusters. (b)S 2p XPS core level spectra of thiophenol capped CdS clusters.

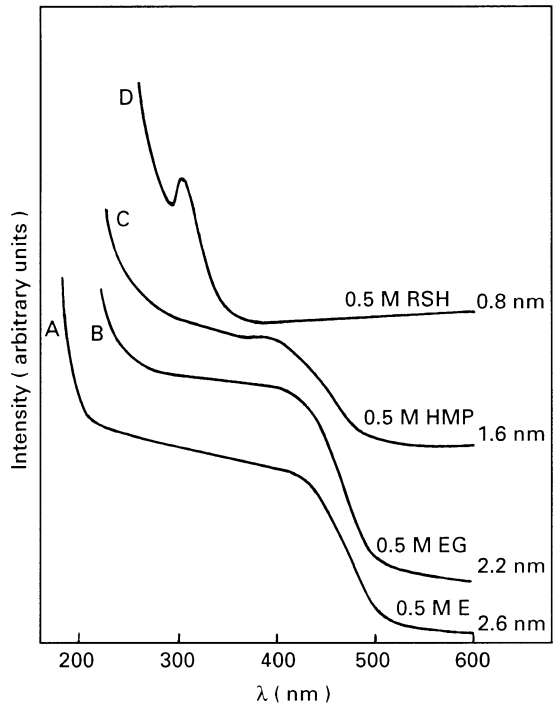


*Figure 7* Optical absorption spectra of CdS clusters obtained by using various additives.

TABLE IV Optical bandgap of CdS clusters obtained by using various additives

| Additive used (0.5 M) | λ (nm) | $E_g$ (eV) |
|---|---|---|
| RSH | 315 | 3.93 |
| HMP | 395 | 3.13 |
| EG | 405 | 3.06 |
| E | 415 | 2.98 |

using HMP, EG and E as the additives, respectively. This means that the CdS nanoclusters obtained are slightly Cd rich, which is expected for Cds under normal synthesis conditions [28]. It was also observed that for 0.8 nm CdS clusters obtained with RSH as the additive, the C/S ratio was 1.74 which indicates that the carbon present in the additive is more than the sulphur content of the CdS nanoclusters (sulphur present in the core of the cluster + the sulphur present in the additive RSH which gets adsorbed on the cluster surface). For 1.6 nm CdS clusters obtained with HMP as the additive, where carbon is not an element of the additive, a low C/S ratio (0.78) was observed as expected. For 2.2 and 2.6 nm clusters with EG and E as additives, C/S ratio was around 2 which was expected as increased carbon content in 2.2 and 2.6 nm clusters was due to the carbon present in ethylene glycol and ethanol, respectively.

It has been discussed earlier that with the increase or decrease of the molarity of the various additives, further shift in the optical absorption spectra was obtained only with RSH as the additive. Also RSH gave the smallest particles, as observed from X-ray diffraction patterns, with narrow size distribution. Hence further experiments have been carried out using RSH as the additive.

### 3.3. Studies of CdS nanocluster with RSH as the additive

In experiments using RSH as the additive two sets of experiments were carried out. In the first set, $CdCl_2$ and $Na_2S$ reagents were kept at a constant molarity of 0.01 M. Studies for this set were done by varying the molarity of RSH additive.

Fig. 11a shows the optical absorption spectra with various concentrations of RSH. It has been observed that as the molarity of RSH increased, the excitonic peak due to quantum size effect shifted to shorter wavelengths thereby increasing the bandgap of the nanoclusters. For a higher concentration of RSH, smaller clusters were obtained as RSH has the property of getting tightly adsorbed on the CdS cluster surface [23, 27]. Hence the size of the CdS nanoclusters can be controlled by varying the concentration of the additives. Table VI gives optical bandgap and the excitonic wavelength position with various concentrations of RSH. Fig. 11b gives the plot of log $M$ versus $E_g$ (eV).

A similar experiment was carried out by varying the $CdCl_2$ and $Na_2S$ molarity by keeping the molarity of RSH constant at 0.5 M. Fig. 12a shows the optical absorption spectra for the same. As expected, with the reduction in $CdCl_2$ and $Na_2S$ molarity the excitonic peak shifted to a shorter wavelength indicating a larger optical bandgap and reduced particle size due to quantum size effects. Table VII lists the excitonic wavelength positions of optical bandgap for the various CdS cluster sizes obtained by the variation of $CdCl_2$ and $Na_2S$ molarity. Fig. 12b shows the plot of log $M$ versus $E_g$ (eV). It can be seen that with the reduction of $CdCl_2$ and $Na_2S$ molarity below 0.001 M the maximum energy gap that can be achieved, is obtained.

Thus for obtaining small clusters, high concentration of RSH is preferred. With a constant value of RSH, a smaller concentration of Cd and S ions also leads to smaller clusters.

With the variation of molarity of the additive RSH from 0.5 to 0.0001 M, particle sizes in the range of 0.8–1.5 nm could be obtained, as observed from XRD patterns (Fig. 13).

XRD studies of the clusters obtained by the variation of Cd and S ion concentration, keeping RSH molarity constant, also showed that the par ticle size varied from 0.8–1.5 nm similar to the first set.

We have carried out systematic ageing studies of CdS nanoclusters obtained with RSH as the additive. Although ageing studies of all the CdS clusters with various molarities of the additive were carried out after 3 days and 10 days, only typical values at 0.5, 0.01 and 0.0001 M RSH additive concentration are presented here. Table VIII gives the excitonic wavelength positions and optical bandgaps for CdS clusters with varying RSH molarity for fresh samples and ageing after 3 and 10 days. Fig. 14a to c shows the optical

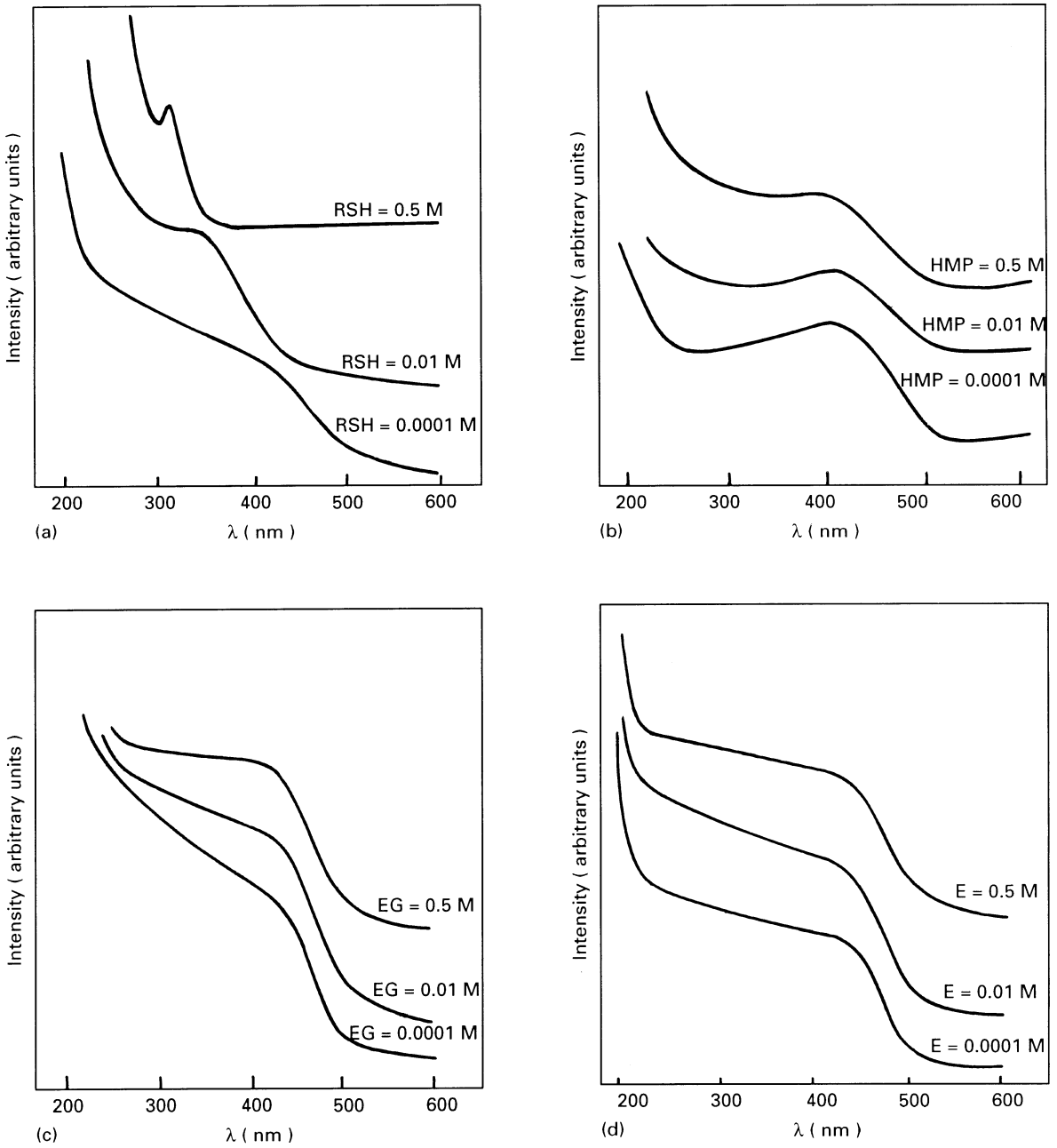


*Figure 8* Optical absorption spectra of CdS clusters obtained by the variation of the molarity of the additives (a) RSH, (b) HMP, (c) EG and (d) E.

absorption spectra for the CdS nanoclusters for the above mentioned conditions.

Fig. 15a to c shows the optical absorption spectra for fresh samples and ageing after 3 and 10 days for CdS clusters obtained by varying the molarity of $CdCl_2$ and $Na_2S$ while keeping the RSH molarity constant at 0.5 M. Here again, although experiments were carried out for all the molarities of $CdCl_2$ and $Na_2S$, however for simplicity, typical molarities of 0.0001, 0.01 and 0.5 M $CdCl_2$ and $Na_2S$ are reported here. Table IX lists the same for fresh samples and ageing after 3 and 10 days.

It is observed from Tables VIII and IX and also from Fig. 14a to c and Fig. 15a to c that ageing of smaller particles with larger bandgaps is comparatively less than larger particles. It was also observed for larger particles [Fig. 14c (0.0001 M RSH) and Fig. 15c (0.5 M $CdCl_2$ and $Na_2S$)] that after ageing, the excitonic peaks become comparatively sharper than the fresh samples, even though they are shifting to larger wavelengths. The shift to larger wavelengths indicates an increase in particle size. But particle size increase and/or aggregation should not produce sharper features on ageing. It has been reported [2, 29] that in homogeneous precipitation the initially formed colloidal crystallites tend to be imperfect and improve in crystallinity with time giving sharper features on ageing. Hence ageing of clusters can be attributed to an increase in particle size and improved perfection of crystallites.

Fig. 13 shows the XRD patterns for RSH capped CdS nanoclusters. It is observed that the smallest 0.8 nm cluster showed a broad diffraction pattern characteristic of an amorphous nature. In correlation

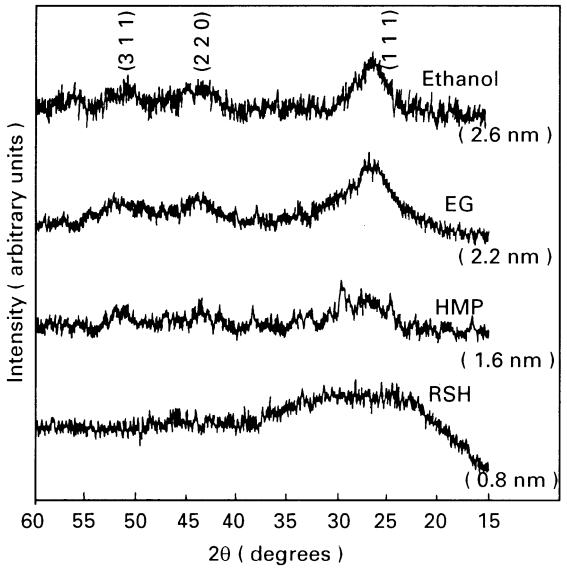


*Figure 9* X-ray diffraction patterns of CdS clusters obtained by using various additives.

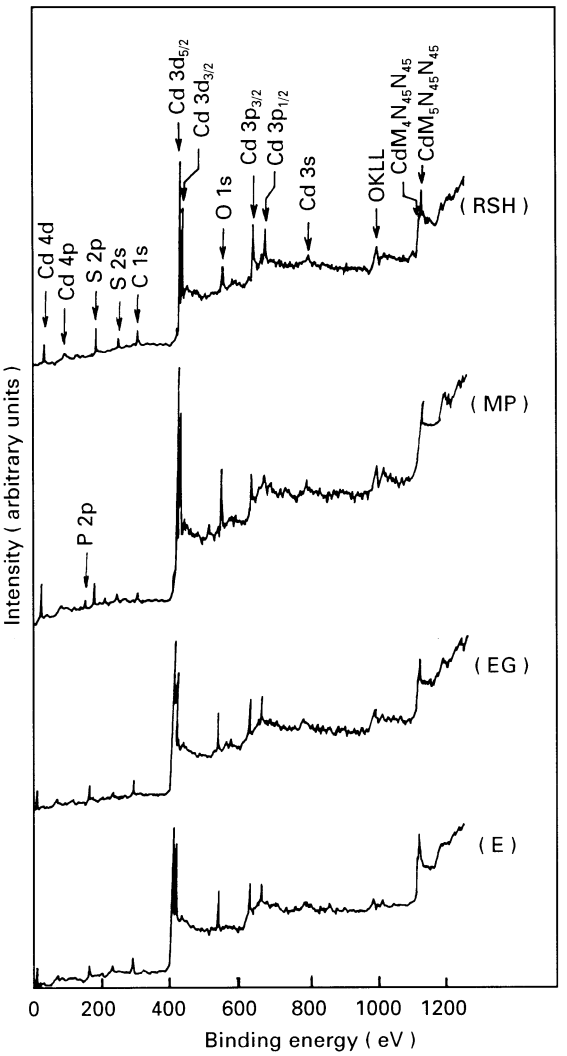


*Figure 10* XPS survey scan of CdS clusters obtained by using various additives.

to this, the electron diffraction pattern for the 0.8 nm (Fig. 16a) CdS clusters showed diffused or broad diffraction rings. As the particle size increased (i.e. 1.5 nm cluster) sharper peaks in XRD patterns (Fig. 13) and sharp rings (Fig. 16b) in electron diffraction patterns were observed indicating improved crystallinity. For 1.5 nm CdS nanoclusters XRD patterns as well as electron diffraction patterns showed (1 1 1), (2 2 0) and (3 1 1) planes characteristic of cubic CdS phase. Thus from diffraction studies it can be concluded that the smallest cluster of CdS is not a cube and intercluster structural long range order does not exist. However smaller clusters maintain tetrahedral geometry.

It has been observed from XRD patterns that for 1.5 nm CdS cluster $2\theta = 27.4^\circ$ which increased to $2\theta = 28.0$ for 0.8 nm cluster thereby showing a contraction in lattice parameter by 3.39 and 5.6 per cent, respectively, with respect to bulk CdS [30].

XPS has again been used for studying the purity of the samples obtained with RSH as the additive. Cd, S, C and O are the elements which were detected. Percentage composition of various elements is shown in Table X for various molarities of RSH along with S/Cd, C/Cd and C/S ratios. As stated earlier, smaller clusters are obtained when higher concentrations of the additive RSH were used. Hence, S/Cd and C/Cd ratios were expected to be higher for smaller clusters. From Table X we see that our experimental observations give similar results.

We carried out detailed investigations of the binding energy core level positions of Cd 3d and S 2p for various particle sizes with RSH as the additive. Fig. 17a and b show Cd 3d and S 2p spectra for various concentrations of RSH. The bulk CdS reference is also shown. Table XI lists the Cd 3d and S 2p peak positions.

It is observed from Table XI that Cd 3d as well as S 2p shift to the higher binding energy side for CdS nanoclusters with respect to bulk CdS. As discussed earlier for thiophenol capped CdS clusters, here again, this may be due to the fact that as the particle size reduces the bandgap increases, increasing the HOMO–LUMO gap, which shifts all the occupied levels to the higher energy side.

TABLE V Concentration of various elements present in the CdS clusters obtained with various additives

| Additive (0.5 M) | Particle size (nm) | Cd (%) | C (%) | S (%) | O (%) | P (%) | S/Cd | C/Cd | C/S |
|---|---|---|---|---|---|---|---|---|---|
| RSH | 0.8 | 16.3 | 43.18 | 24.8 | 15.72 | — | 1.52 | 2.87 | 1.74 |
| HMP | 1.6 | 21.25 | 13.7 | 17.5 | 34.71 | 12.7 | 0.82 | 0.64 | 0.78 |
| EG | 2.2 | 19.05 | 31.49 | 16.06 | 33.38 | — | 0.84 | 1.73 | 1.96 |
| E | 2.6 | 17.19 | 30.8 | 15.86 | 36.19 | — | 0.91 | 1.79 | 1.95 |

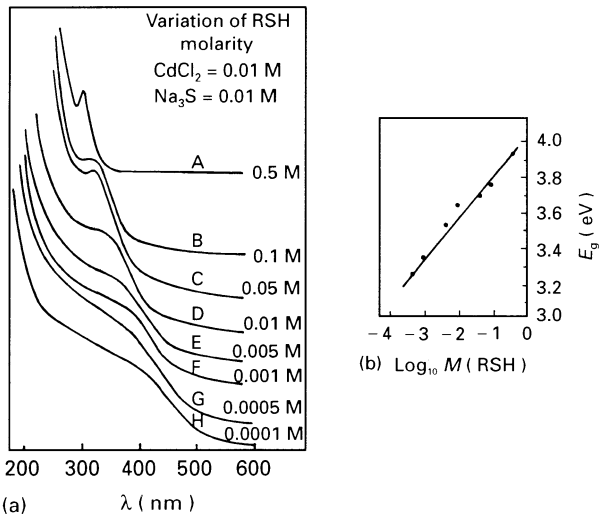


*Figure 11* (a) Optical absorption spectra of CdS clusters obtained by the variation of the molarity of the additive RSH keeping $CdCl_2$ and $Na_2S$ molarity constant at 0.01 M. (b) Plot of energy gap versus log *M*.

TABLE VI Optical band gap of CdS clusters obtained by the variation of concentration of the additive RSH keeping $CdCl_2$ and $Na_2S$ at a constant molarity of 0.01 M

| RSH molarity (M) | λ (nm) | $E_g$ (eV) |
|---|---|---|
| 0.5 | 315 | 3.93 |
| 0.1 | 330 | 3.78 |
| 0.05 | 335 | 3.70 |
| 0.01 | 340 | 3.64 |
| 0.005 | 350 | 3.54 |
| 0.001 | 370 | 3.35 |
| 0.0005 | 380 | 3.26 |
| 0.0001 | 390 | 3.17 |

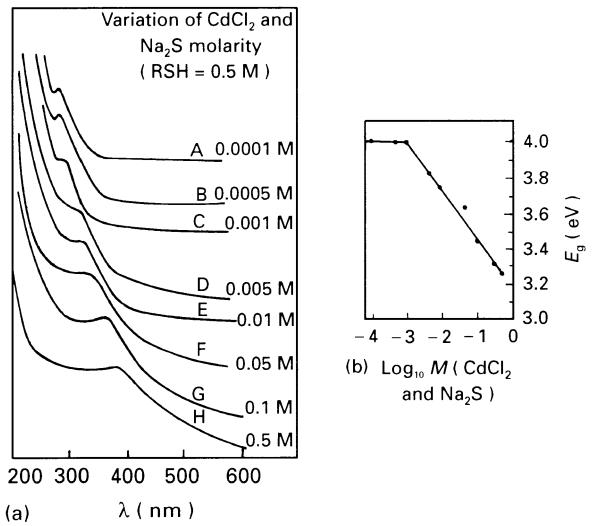


*Figure 12* (a) Optical absorption spectra of CdS clusters obtained by the variation of $CdCl_2$ and $Na_2S$ molarities keeping additive RSH at 0.5 M. (b) Plot of energy gap versus log *M*.

Thus, with RSH as the additive, CdS nanoclusters as small as 0.8 nm have been synthesized and studied in detail. Systematic ageing studies showed that larger particles age faster than the smaller clusters. XPS has been found to be a very useful tool in finding the purity and stoichiometry of the nanoclusters and it supports the existing proposal of the formation of CdS nanoclusters by chemical synthesis.

TABLE VII Optical bandgap of CdS clusters obtained by the variation of concentration of $CdCl_2$ and $Na_2S$ keeping additive RSH at a constant molarity of 0.5 M

| $CdCl_2$ and $Na_2S$ molarity (M) | λ (nm) | $E_g$ (eV) |
|---|---|---|
| 0.0001 | 310 | 4.0 |
| 0.0005 | 310 | 4.0 |
| 0.001 | 310 | 4.0 |
| 0.005 | 325 | 3.81 |
| 0.01 | 330 | 3.75 |
| 0.05 | 340 | 3.64 |
| 0.1 | 360 | 3.44 |
| 0.5 | 380 | 3.26 |

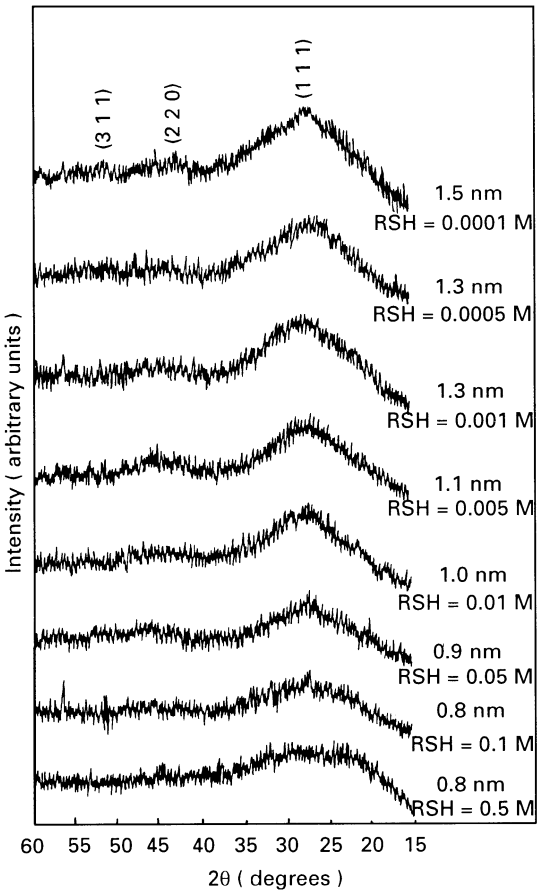


*Figure 13* X-ray diffraction patterns for CdS clusters with various molarities of the additive RSH.

## 4. Conclusions

We have been successful in synthesizing CdS nanoclusters by aqueous and non-aqueous chemical methods. In the non-aqueous method, thiophenol was used as an additive whereas for the aqueous method of synthesis four different additives, i.e. mercaptoethanol, hexametaphosphate, ethylene glycol and ethanol,

TABLE VIII Ageing studies of CdS clusters obtained with various molarities of the additive RSH.

| Variation of RSH molarity (M) | Fresh | | 3 days | | 10 days | |
|---|---|---|---|---|---|---|
| | λ (nm) | $E_g$ (eV) | λ (nm) | $E_g$ (eV) | λ (nm) | $E_g$ (eV) |
| 0.5 | 315 | 3.93 | 320 | 3.87 | 320 | 3.87 |
| 0.01 | 340 | 3.64 | 355 | 3.49 | 360 | 3.44 |
| 0.0001 | 390 | 3.17 | 395 | 3.13 | 415 | 2.98 |

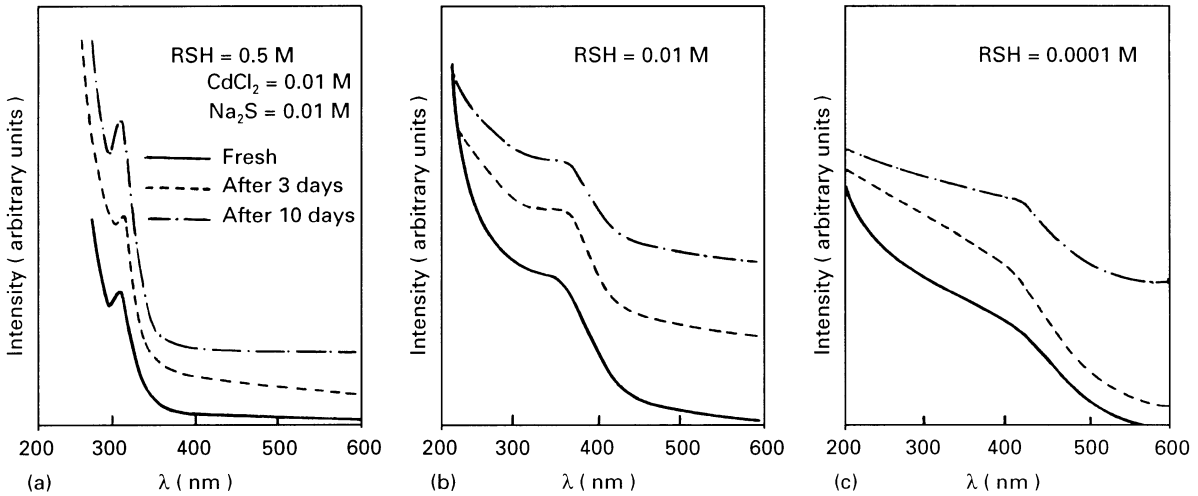


*Figure 14* Optical absorption spectra for studying ageing effect of CdS clusters with variation of RSH molarity.

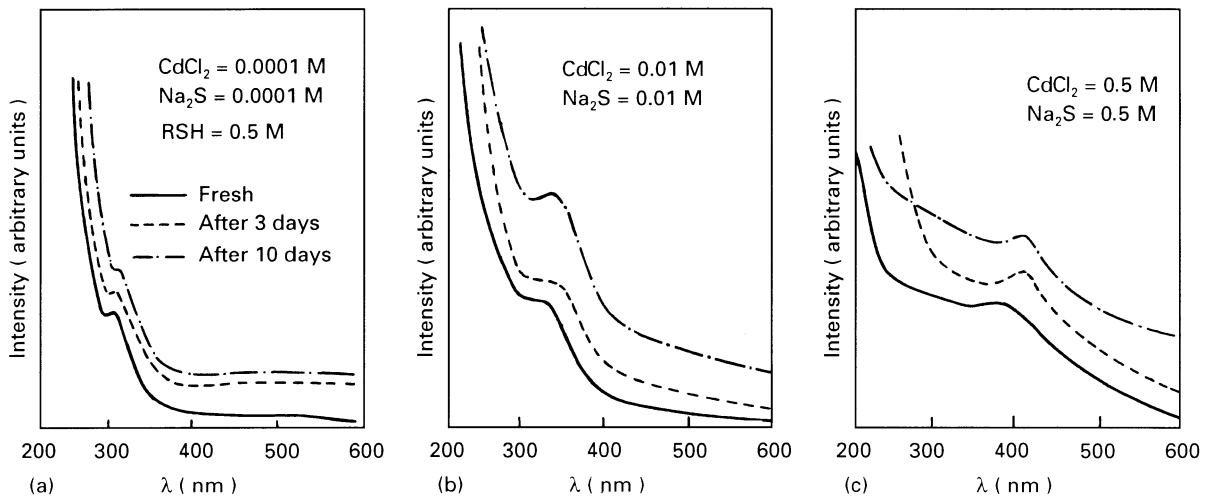


*Figure 15* Optical absorption spectra for ageing effect studies with variation of molarities of $CdCl_2$ and $Na_2S$ reagents.

TABLE IX Ageing studies of CdS clusters obtained with various molarities of $CdCl_2$ and $Na_2S$

| Variation of $CdCl_2$ and $Na_2S$ molarity (M) | Fresh | | 3 days | | 10 days | |
|---|---|---|---|---|---|---|
| | λ (nm) | $E_g$ (eV) | λ (nm) | $E_g$ (eV) | λ (nm) | $E_g$ (eV) |
| 0.0001 | 310 | 4.0 | 315 | 3.93 | 320 | 3.87 |
| 0.01 | 330 | 3.75 | 340 | 3.64 | 345 | 3.59 |
| 0.5 | 380 | 3.26 | 410 | 3.02 | 410 | 3.02 |

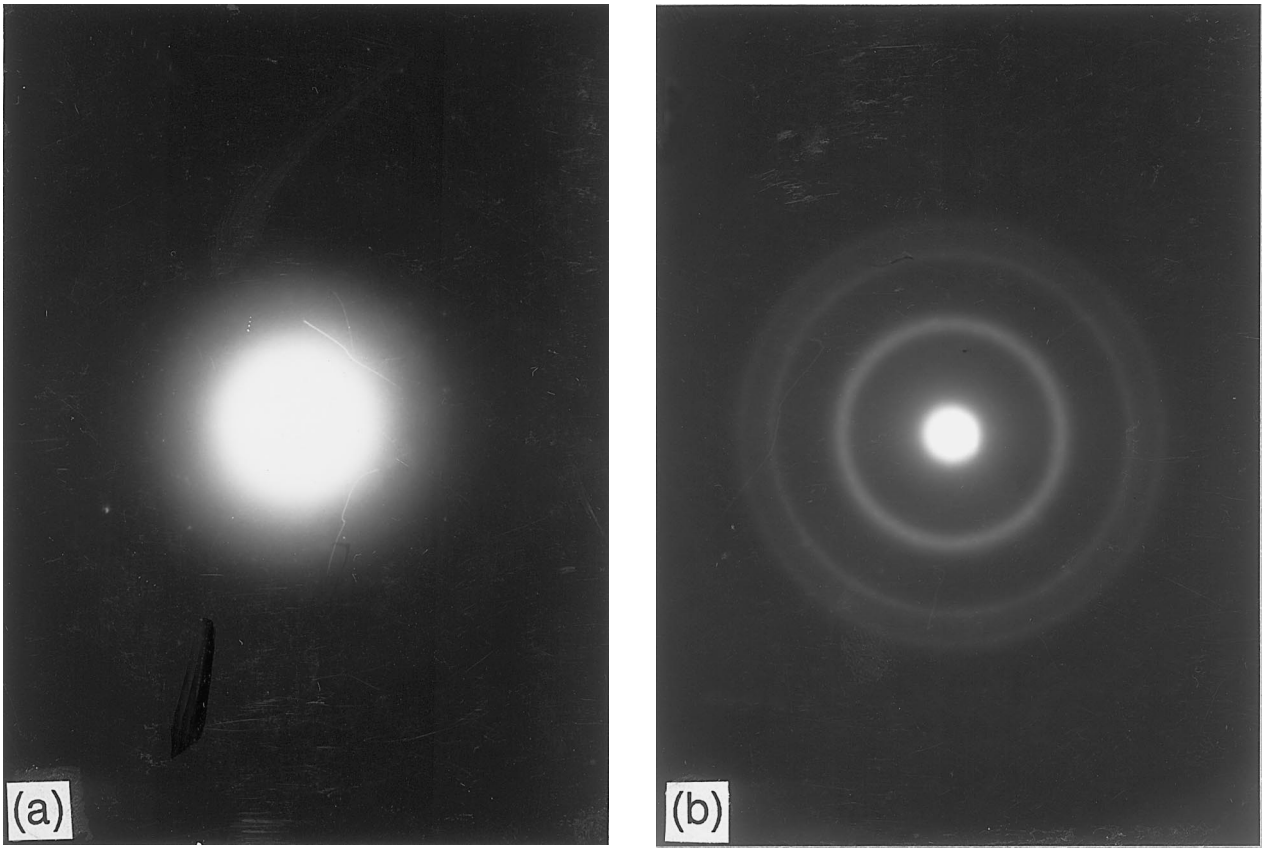


*Figure 16* Electron diffraction patterns for (a) 0.8 nm and (b) 1.5 nm RSH capped CdS clusters.

TABLE X Concentration of various elements present in the CdS clusters obtained with various molarities of the additive RSH

| RSH molarity (M) | Particle size (nm) | Cd (%) | C (%) | S (%) | O (%) | S/Cd | C/Cd | C/S |
|---|---|---|---|---|---|---|---|---|
| 0.5 | 0.8 | 16.3 | 43.18 | 24.8 | 15.72 | 1.52 | 2.87 | 1.74 |
| 0.01 | 1.0 | 19.1 | 42.65 | 24.2 | 14.05 | 1.26 | 2.23 | 1.76 |
| 0.0001 | 1.5 | 21.06 | 42.12 | 24.2 | 12.62 | 1.149 | 2.00 | 1.74 |

were used. The following conclusions can be made for the CdS nanoclusters synthesized and studied by us.

1. Particles as small as 0.7 nm with a very narrow size distribution could be achieved with thiophenol as the additive. Optical bandgap of 4.59 eV is obtained which is the largest bandgap obtained to date for this material by chemical synthesis.

2. When mercaptoethanol was used as an additive CdS clusters with optical bandgap of 4.0 eV were obtained. With hexametaphosphate, ethylene glycol and ethanol used as the additives, optical bandgaps of 3.13, 3.06 and 2.98 eV for CdS nanoclusters could be achieved.

3. Particle size could be controlled and hence a variation in the optical bandgap could be obtained by varying the molarity of the additives thiophenol and RSH. However, with the variation in molarity of the additives HMP, EG and E, no further change in the optical bandgap of CdS nanoclusters could be observed.

4. The smallest 0.7 nm clusters are amorphous in nature. However as the particle size increased, cubic phase was observed.

5. Systematic ageing studies indicated that the small clusters ( $\sim 0.7$ nm) hardly showed any ageing effect. But bigger clusters ( $\sim 2.0$ nm) showed a red shift in the optical absorption spectra. Ageing also leads to better crystallization of the particles.

6. Clusters synthesized were highly pure in nature.

7. The smallest 0.7 nm cluster may have a molecular structure of $[Cd_{10}S_4(SPh)_{16}]^{4-}$ (from XPS measurements).

8. Cd 3d and S 2p XPS core levels of the clusters showed a shift to the higher binding energy side which may be due to the increase in bandgap of the clusters and a corresponding shift of all occupied levels to higher energies.

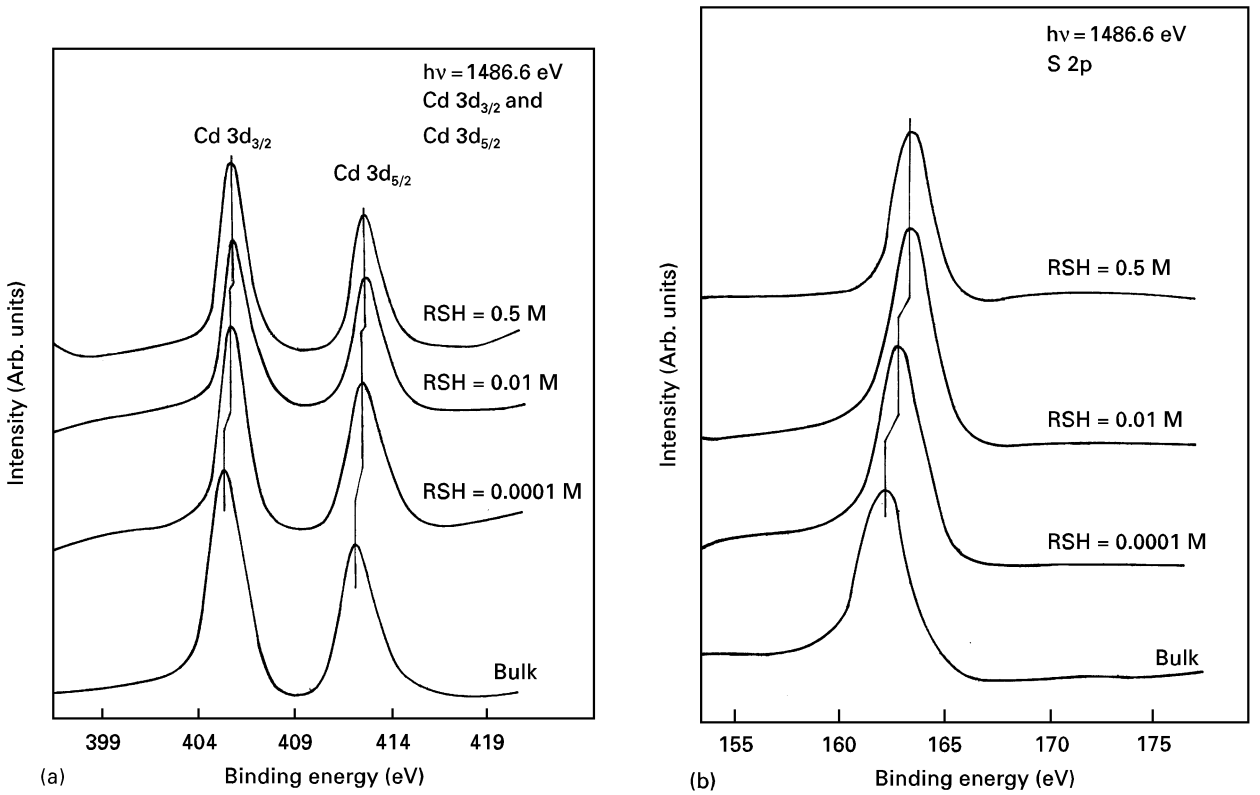


*Figure 17* (a) Cd 3d XPS core level spectra for CdS clusters of various sizes obtained with the variation of the molarity of RSH. (b) S 2p XPS core level spectra for RSH capped CdS nanoclusters.

TABLE XI Cd 3d and S 2p XPS core level positions of CdS clusters obtained with various molarities of the additive RSH

| Molarity of RSH (M) | Particle size (nm) | Cd $3d_{5/2}$ (eV) | Cd $3d_{3/2}$ (eV) | S 2p (eV) |
|---|---|---|---|---|
| – | Bulk | 405.3 | 412.1 | 162.1 |
| 0.0001 | 1.5 | 405.95 | 412.7 | 162.7 |
| 0.01 | 1.0 | 406 | 412.75 | 162.95 |
| 0.5 | 0.8 | 406 | 412.75 | 162.95 |


## Acknowledgements

S.K.K would like to thank University Grants Commission, India, and M.K. would like to thank Council of Scientific and Industrial Research, India, for financial support.


## References


1. L.E. BRUS, *J. Chem. Phys.* **79** (1983) 5566.
2. R. ROSSETTI, R. HULL, J.M. GIBSON and L.E. BRUS, *ibid.* **82** (1985) 552.
3. A. FOJTIK, H. WELLER and A. HENGLIEN, *Chem. Phys. Lett.* **120** (1985) 552.
4. J.G. TOBIN, V.L. COLVIN and A.P. ALIVISATOS, *J. Vac. Sci. Tech.* **A9** (1991) 852.
5. N. HERRON, Y. WANG and H. ECKERT, *J. Amer. Chem. Soc.* **112** (1990) 1322.
6. A. ROY, D.D. SARMA and A.K. SOOD, *Spectrochemica Acta*, **48A** (1992) 1779.
7. S. MAHAMUNI, A.A. KHOSRAVI, M. KUNDU, A. KSHIRSAGAR, A. BEDEKAR, D.B. AVASARE, P. SINGH and S.K. KULKARNI, *J. Appl. Phys.* **73** (1993) 5237.
8. L.E. BRUS, *J. Chem. Phys.* **80** (1984) 4403.
9. Y. WANG and N. HERRON, *J. Phys. Chem.* **95** (1991) 525.
10. A. HENGLIEN, *Top. Curr. Chem.* **143** (1988) 113.
11. R.P. ANDRES, R.S. AVERBACK, W.L. BROWN, L.E. BRUS, W.A. GODDARD, K. KALDOR, S.G. LOUIE, M. MOSCOVITS, P.S. PEERCY, S.J. RILEY, R.W. SEIGEL, F. SPAEPEN and Y. WANG, *J. Mater. Res.* **4** (1989) 704.
12. M.G. BAWENDI, M.L. STEIGERWALD and L.E. BRUS, *Ann. Rev. Phys. Chem.* **41** (1990) 477.
13. E. HILINSKI, P. LUCAS and Y. WANG, *J. Chem. Phys.* **89** (1988) 3435.
14. Y. WANG, and N. HERRON, *J. Phys. Chem.* **91** (1987) 257.
15. M. MEYER, C. WALLBERG, K. KURIHARA and J.H. FENDLER, *J. Chem. Soc. Chem. Commun.* (1984) 90.
16. P. LINAOS and J.K. THOMAS, *Chem. Phys. Lett.* **125** (1986) 299.
17. M.P. PILENI, I. LISIECKI, L. MOTTE and C. PETIT, *Res. Chem. Intermed.* **17** (1992) 101.
18. R.R. CHANDLER, J.L. COFFER, S.J. ATHERTON and P.J. SNOWDEN, *J. Phys. Chem.* **96** (1992) 2713.
19. J.J. SHIANG, S.H. RISBUD and A.P. ALIVISATOS, *J. Chem. Phys.* **98** (1993) 8432.
20. N.F. BORRELLI, D.W. HALL, H.J. HOLLAND and D.W. SMITH, *J. Appl. Phys.* **61** (1987) 5399.
21. L.C. LIU and S.H. RISBUD, *ibid.* **68** (1990) 28.
22. I.G. DANCE, A. CHOY and M.L. SCUDDER, *J. Amer. Chem. Soc.* **106** (1984) 6285.
23. Y. NOSAKA, K. YAMAGUCHI, H. MIYAMA and M. HAYASHI, *Chem. Lett.* (1988) 605.
24. Y. WANG and N. HERRON, *Phys. Rev.* **B42** (1990) 7253.
25. A. TAYLOR, "X-ray metallography" (Wiley, New York, 1961).

26. J.R. SACHLEBEN, E.W. WOOTEN, L. EMSLEY, A. PINES, V.L. COLVIN and A.P. ALIVISATOS, *Chem. Phys. Lett*. **198** (1992) 431.
27. M.J. NATAN, J.W. THAKERAY and M.S. WRIGHTON, *J. Phys. Chem.* **90** (1986) 4089.
28. M. SAVELLI and J. BOUGNOT, *Topics in Appl. Phys.* **31**, (Springer Verlag, Berlin, 1979).
29. I.M. KOLTHOFF, E.B. SANDELL, E.J. MEEHAN and S. BRUCKENSTEIN, "Quantitative chemical analysis" 4th Edn (Macmillan, London, 1969) Ch. 10.
30. ASTM data cards : CdS : 10 -454.

*Received 11 January*
*and accepted 11 May 1995*